



PERGAMON

Journal of Quantitative Spectroscopy &
Radiative Transfer 70 (2001) 663–673

Journal of
Quantitative
Spectroscopy &
Radiative
Transfer

www.elsevier.com/locate/jqsrt

T-matrix method for electromagnetic scattering from scatterers with complex structure

Adrian Doicu, Thomas Wriedt*

Institut für Werkstofftechnik, Badgasteiner Strasse 3, 28359 Bremen, Germany

Abstract

We describe a T-matrix program for light scattering calculations from particles with complex structure. The code treats the cases of homogeneous, layered and composite scatterers. These results are combined with basic results concerning the scattering by inhomogeneous scatterers and aggregates to apply to more general types of scatterers. Some numerical simulations are presented. © 2001 Elsevier Science Ltd. All rights reserved.

Keywords: T-matrix method; Null-field method; Extended boundary condition method; Discrete sources method; Composite scatterers; Aggregated scatterers

1. Introduction

One of the fastest and most powerful numerical tools for computing nonspherical light scattering using localized vector spherical functions is the T-matrix method originally developed by Waterman [1]. This method has recently been reviewed in a book chapter by Mishchenko et al. [2]. The T-matrix is independent of the incident and scattered fields and depend only on the shape, size parameter, and refractive index of the scattering particle as well as on its orientation with respect to the coordinate system. However, for particles with extreme geometries or particles with appreciable concavities the single spherical coordinate based null-field method fails to converge. A number of modifications to the conventional null-field method have been suggested to improve the numerical stability. These techniques include formal modifications of the single spherical coordinate based null-field method [3,4], different choices of basis functions

* Corresponding author. Tel.: +49-421-218-2507; fax: +49-421-218-5378.

E-mail address: thw@iwt.uni-bremen.de (T. Wriedt).

[5,6] and the application of the spheroidal coordinate formalism [7,8]. Another formal modification is the null-field method with discrete sources [9,10]. Essentially, this method entails the use of a number of elementary sources for approximating the surface current densities. The discrete sources are placed on a certain support in an additional region with respect to the region where the solution is required. Unknown discrete source amplitudes which produces the surface densities are computed by using the null-field condition of the total electric field inside the particle surface. Discrete sources were used in the iterative version of the null-field method [6]. The iterative method utilizes multiple spherical expansions to represent the internal fields in different overlapping regions, rather than summing up the various expansions and using it throughout the particle as in the discrete sources method. The various expansions are matched in the overlapping regions to enforce the continuity of the fields throughout the entire interior volume.

The T-matrix formalism with discrete sources can be extended in a simple manner for composite and layered particles. In this context, the earlier results [11–13] on the T-matrix method concerning the scattering of an arbitrarily shaped particle with a nonconcentric, arbitrarily shaped inclusion or the scattering by an arbitrary number of scatterers, can be combined with these new results to apply to more general types of scattering problems.

2. Computation of the T-matrix

2.1. Homogeneous scatterer

The null-field method with discrete sources for homogeneous scatterers was described by Doicu et al. [10]. For solving the transmission boundary-value problem in the framework of the null-field method with discrete sources, the scattering object is replaced by a set of surface current densities, so that in the exterior domain the sources and fields are exactly the same as those existing in the original scattering problem. A set of integral equations for the surface current densities is derived for a variety of discrete sources. Physically, the set of integral equations in question guarantees the null-field condition inside the particle. It is noted that the localized and distributed vector spherical functions, magnetic and electric dipoles or vector Mie-potentials can be used as discrete sources. The surface current densities are then approximated by fields of discrete sources corresponding to the internal problem. Once the surface current densities are determined, the scattered field outside the circumscribing sphere is obtained by using the representation theorem. Finally, the transition matrix is obtained by assuming spherical vector wave expansions for the incident and the scattered field [14].

2.2. Composite scatterer

We consider the generic case of a composite scatterer that consists of two different homogeneous regions, D_1 and D_2 . The geometry of the scatterer is shown in Fig. 1. The surface between the domains D_1 and D_2 is denoted by S_{12} . Besides the common origin O , there is one local origin O_i in each homogeneous region D_i . The two homogeneous regions are characterized

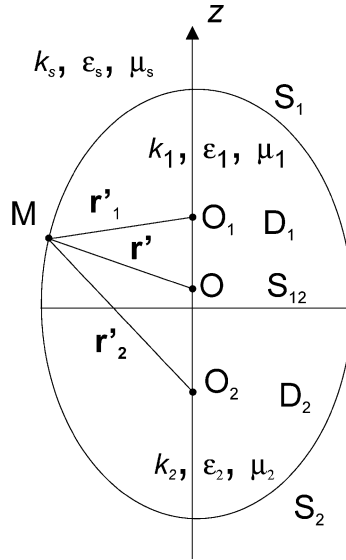


Fig. 1. Geometry of a composite scatterer.

by the relative electric permittivities ϵ_i and the relative magnetic permeabilities μ_i , where $i=1, 2$. The corresponding wave numbers are $k_i = k\sqrt{\epsilon_i\mu_i}$, $i = 1, 2$, while the wave number for the free space is $k_s = k\sqrt{\epsilon_s\mu_s}$, with $k = \omega/c$.

Let us rewrite the basic equations of the conventional null-field method in a slightly different form as given by Peterson and Ström [12]. By considering the null-field conditions for the total electric field within D_i , we obtain the following set of integral equations for the surface current densities

$$\sum_{j=1}^2 \int_{S_j \cup S_{12}} \left[\mathbf{e}_j^{\mathcal{N}}(\mathbf{r}'_j) - \mathbf{e}_0(\mathbf{r}'_j) \right] \begin{pmatrix} \mathbf{N}_{-mn}^3(k_s \mathbf{r}'_i) \\ \mathbf{M}_{-mn}^3(k_s \mathbf{r}'_i) \end{pmatrix} + j \sqrt{\frac{\mu_s}{\epsilon_s}} \left[\mathbf{h}_j^{\mathcal{N}}(\mathbf{r}'_j) - \mathbf{h}_0(\mathbf{r}'_j) \right] \begin{pmatrix} \mathbf{N}_{-mn}^3(k_s \mathbf{r}'_i) \\ \mathbf{M}_{-mn}^3(k_s \mathbf{r}'_i) \end{pmatrix} \right] dS(\mathbf{r}'_j) = 0, \quad (1)$$

where $i = 1, 2$, $m = -M, \dots, M$ and $n = |m|, \dots, N$. Here, we denote by $\mathbf{e}_j, \mathbf{h}_j$ the surface current densities on the closed surface $S_j \cup S_{12}$ and by $\mathbf{e}_0, \mathbf{h}_0$ the tangential components of the incident electric and magnetic field, respectively. Note, the continuity conditions $\mathbf{e}_1 = \mathbf{e}_2$ and $\mathbf{h}_1 = \mathbf{h}_2$ on S_{12} . The index \mathcal{N} is a complex index incorporating M and N . In the conventional method, the surface integrals containing the tangential components of the incident field are identified as the expansion coefficients of the external excitation in terms of the regular spherical vector wave functions.

An approximate solution to the scattering problem can be obtained by approximating the surface current densities by the complete set of tangential, single spherical coordinate vector

wave functions

$$\begin{aligned}
 \begin{pmatrix} \mathbf{e}_j^{\mathcal{N}}(\mathbf{r}'_j) \\ \mathbf{h}_j^{\mathcal{N}}(\mathbf{r}'_j) \end{pmatrix} &= \sum_{m=-M}^M \sum_{n=|m|}^N a_{mn}^{j,\mathcal{N}} \begin{pmatrix} \mathbf{n} \times \mathbf{M}_{mn}^1(k_j \mathbf{r}'_j) \\ -j \sqrt{\frac{\epsilon_j}{\mu_j}} \mathbf{n} \times \mathbf{N}_{mn}^1(k_j \mathbf{r}'_j) \end{pmatrix} \\
 &+ b_{mn}^{j,\mathcal{N}} \begin{pmatrix} \mathbf{n} \times \mathbf{N}_{mn}^1(k_j \mathbf{r}'_j) \\ -j \sqrt{\frac{\epsilon_j}{\mu_j}} \mathbf{n} \times \mathbf{M}_{mn}^1(k_j \mathbf{r}'_j) \end{pmatrix}. \tag{2}
 \end{aligned}$$

The above formalism can be modified by replacing the set of single spherical coordinate vector wave functions $\{\mathbf{M}_{mn}^{1,3}(k\mathbf{r}_i), \mathbf{N}_{mn}^{1,3}(k\mathbf{r}_i)\}_{m \in \mathbb{Z}, n=|m|, \dots}$ by the system lowest-order spherical vector wave functions $\{\mathbf{M}_{m,|m|+l}^3[k(\mathbf{r}_i - z_p^i \mathbf{e}_3)], \mathbf{N}_{m,|m|+l}^3[k(\mathbf{r}_i - z_p^i \mathbf{e}_3)]\}_{m \in \mathbb{Z}, p=1,2, \dots}$, where $(\mathbf{e}_1, \mathbf{e}_2, \mathbf{e}_3)$ are the unit vectors in Cartesian coordinates, $(z_p^i)_{p=1,2, \dots}$ is a dense sequence of points on a segment Γ_z^i of the z -axis, $\Gamma_z^i \subset D_i$, and $l = 1$ if $m = 0$ and $l = 0$ otherwise. By employing the same arguments as given by Doicu et al. [10] we can show that the set of integral equations (1) written in terms of distributed lowest-order spherical vector wave functions guarantees the null-field condition within D_i . An approximate solution to the scattering problem may be written as a linear combination of the distributed spherical vector wave functions. The transition matrix for the composite scatterer can be obtained by following the same strategy as in the homogeneous case [14]. The advantage of using the system of lowest-order spherical vector wave functions as a system of discrete sources is that for axisymmetric scatterers the problem decouples over the azimuthal modes m . In the case of prolate scatterers, the choice of the multipoles on the axis of symmetry adequately describes the particle geometry. This arrangement is not suitable for oblate scatterers. In this case, the procedure of an analytic continuation of the representation of the spherical vector-wave functions onto the complex plane along the source coordinate z should be employed [15]. As it was shown in a previous paper [16], the use of distributed sources extend the domain of applicability of the null-field method to highly elongated and flattened composite scatterers.

2.3. Multilayered scatterer

We consider the generic case of a two-layered scatterer defined by the closed surfaces S_1 and S_2 , where S_1 encloses S_2 according to Fig. 2. The exterior of S_1 is denoted by D_s , the interior of S_2 by D_2 and the domain between S_1 and S_2 by D_1 . The local origin O_i is attached to the closed surface S_i . The wave number of the domain D_i is $k_i = k \sqrt{\epsilon_i \mu_i}$, where $i = s, 1, 2$.

The basic equations for the conventional null-field method can be obtained by applying the equivalence principle which reduces the two-layered scattering problem into three subproblems. For each subproblem, surface current densities are set up to create the actual field in the region of interest and a null field elsewhere. Let $\mathbf{e}_j, \mathbf{h}_j$ be the surface current densities acting on the closed surface S_j . For the subproblem corresponding to the exterior domain D_s , we consider the null-field condition inside an inscribed sphere of S_1 . This leads to the following set of integral

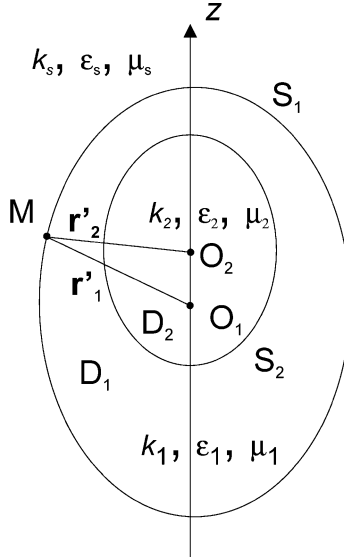


Fig. 2. Geometry of a layered scatterer.

equations for the surface current densities \mathbf{e}_1 and \mathbf{h}_1 :

$$\int_{S_1} \left[[\mathbf{e}_1^{\mathcal{N}}(\mathbf{r}'_1) - \mathbf{e}_0(\mathbf{r}'_1)] \begin{pmatrix} \mathbf{N}_{-mn}^3(k_s \mathbf{r}'_1) \\ \mathbf{M}_{-mn}^3(k_s \mathbf{r}'_1) \end{pmatrix} + j \sqrt{\frac{\mu_s}{\varepsilon_s}} [\mathbf{h}_1^{\mathcal{N}}(\mathbf{r}'_1) - \mathbf{h}_0(\mathbf{r}'_1)] \begin{pmatrix} \mathbf{N}_{-mn}^3(k_s \mathbf{r}'_1) \\ \mathbf{M}_{-mn}^3(k_s \mathbf{r}'_1) \end{pmatrix} \right] dS(\mathbf{r}'_1) = 0. \quad (3)$$

For the subproblem corresponding to the domain D_1 , we consider the null-field conditions outside a circumscribed sphere of S_1 and inside an inscribed sphere of S_2 . The resulting system of integral equations relates the surface current densities \mathbf{e}_1 and \mathbf{h}_1 to \mathbf{e}_2 and \mathbf{h}_2 , that is,

$$\sum_{j=1}^2 (-1)^j \int_{S_j} \left[\mathbf{e}_j^{\mathcal{N}}(\mathbf{r}'_j) \begin{pmatrix} \mathbf{N}_{-mn}^{1,3}(k_1 \mathbf{r}'_j) \\ \mathbf{M}_{-mn}^{1,3}(k_1 \mathbf{r}'_j) \end{pmatrix} + j \sqrt{\frac{\mu_1}{\varepsilon_1}} \mathbf{h}_j^{\mathcal{N}}(\mathbf{r}'_j) \begin{pmatrix} \mathbf{N}_{-mn}^{1,3}(k_1 \mathbf{r}'_j) \\ \mathbf{M}_{-mn}^{1,3}(k_1 \mathbf{r}'_j) \end{pmatrix} \right] dS(\mathbf{r}'_j) = 0 \quad (4)$$

for $i=1, 2$, $m=-M, \dots, M$ and $n=|m|, \dots, N$. Regular spherical vector wave functions are taken as testing functions in the case $i=1$, while radiating spherical vector wave functions are taken in the case $i=2$.

The surface current densities \mathbf{e}_1 and \mathbf{h}_1 are approximated by a linear combination of the tangential components of the regular and radiating single spherical coordinate vector wave functions. For representing the surface current densities \mathbf{e}_2 and \mathbf{h}_2 , we use only regular functions.

In a compact notation we may write

$$\begin{pmatrix} \mathbf{e}_j^{\mathcal{N}}(\mathbf{r}'_j) \\ \mathbf{h}_j^{\mathcal{N}}(\mathbf{r}'_j) \end{pmatrix} = \sum_{m=-M}^M \sum_{n=|m|}^N a_{mn}^{j,\mathcal{N}} \begin{pmatrix} \mathbf{n} \times \mathbf{M}_{mn}^1(k_j \mathbf{r}'_j) \\ -j \sqrt{\frac{\epsilon_j}{\mu_j}} \mathbf{n} \times \mathbf{N}_{mn}^1(k_j \mathbf{r}'_j) \end{pmatrix} + b_{mn}^{j,\mathcal{N}} \begin{pmatrix} \mathbf{n} \times \mathbf{N}_{mn}^1(k_j \mathbf{r}'_j) \\ -j \sqrt{\frac{\epsilon_j}{\mu_j}} \mathbf{n} \times \mathbf{M}_{mn}^1(k_j \mathbf{r}'_j) \end{pmatrix} \\ + \delta_{j1} \left[c_{mn}^{j,\mathcal{N}} \begin{pmatrix} \mathbf{n} \times \mathbf{M}_{mn}^3(k_j \mathbf{r}'_j) \\ -j \sqrt{\frac{\epsilon_j}{\mu_j}} \mathbf{n} \times \mathbf{N}_{mn}^3(k_j \mathbf{r}'_j) \end{pmatrix} + d_{mn}^{j,\mathcal{N}} \begin{pmatrix} \mathbf{n} \times \mathbf{N}_{mn}^3(k_j \mathbf{r}'_j) \\ -j \sqrt{\frac{\epsilon_j}{\mu_j}} \mathbf{n} \times \mathbf{M}_{mn}^3(k_j \mathbf{r}'_j) \end{pmatrix} \right], \tag{5}$$

where δ_{ji} is the Kronecker symbol. As in the case of composite scatterers, the above formalism can be modified by replacing the set of single spherical coordinate vector wave functions by the set of lowest-order spherical vector wave functions. In this case, the sequences of dense points $(z_p^1)_{p=1,2,\dots}$ and $(z_p^2)_{p=1,2,\dots}$ are located in the interior of S_1 and S_2 , respectively. For computing the transition matrix, we approximate the surface current densities \mathbf{e}_1 and \mathbf{h}_1 by fields of regular and radiating distributed sources, while the densities \mathbf{e}_2 and \mathbf{h}_2 are approximated by fields of regular distributed sources. The numerical analysis given in a previous paper [17] demonstrates the efficiency of using distributed sources in electromagnetic scattering from layered particles with extreme geometries.

2.4. Scatterers with arbitrarily shaped inclusions and systems of scatterers

By invoking the results of the precedent sections and relying on the formulations of Peterson and Ström [11,12], we may compute the total transition matrices for some complex structures. For a system of two particles as depicted in Fig. 3a we have

$$\begin{aligned} \mathbf{T}_{12} = & \sigma_{O_1}^1 \mathbf{T}_1 [\mathbf{I} - \sigma_{O_1 O_2}^3 \mathbf{T}_2 \sigma_{O_2 O_1}^3 \mathbf{T}_1]^{-1} [\sigma_{O_1 O_2}^3 \mathbf{T}_2 \sigma_{O_2 O}^1 + \sigma_{O_1 O}^1] \\ & + \sigma_{O_2 O}^1 \mathbf{T}_2 [\mathbf{I} - \sigma_{O_2 O_1}^3 \mathbf{T}_1 \sigma_{O_1 O_2}^3 \mathbf{T}_2]^{-1} [\sigma_{O_2 O_1}^3 \mathbf{T}_1 \sigma_{O_1 O}^1 + \sigma_{O_2 O}^1], \tag{6} \end{aligned}$$

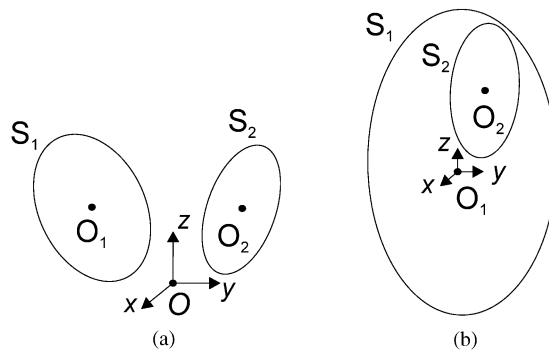


Fig. 3. Geometry of (a) a system of scatterers, and (b) a scatterer with an arbitrarily shaped inclusion.

where \mathbf{T}_1 and \mathbf{T}_2 stand for the transition matrices of the scatterers bounded by the surfaces S_1 and S_2 , respectively, and $\sigma_{OO_1}^{1,3}$ are the rototranslation matrices passing from the origin O to the origin O_1 . The most interesting feature of Eq. (6) is that the total T-matrix is expressed in terms of T-matrices of individual scatterers. These transition matrices incorporate all informations concerning the optical and geometrical characteristics of the particles. For three or more scatterers it is difficult to give an explicit expression for the total T-matrix, but the mathematical model involves only the individual T-matrices of each scatterer. From the analysis given by Peterson and Ström [11,12] it is clear that the scatterers can be multilayered or composite. The corresponding transition matrices may be computed according to the discussion in Sections 2.2 and 2.3.

The transition matrix of a scatterer containing an arbitrarily shaped inclusion as shown in Fig. 3b is given by

$$\mathbf{T}_{12} = [\mathbf{T}_1 - \mathbf{Q}_1^{1,3} \hat{\mathbf{T}}_2 (\mathbf{Q}_1^{3,1})^{-1}] [\mathbf{I} - \mathbf{Q}_1^{3,3} \hat{\mathbf{T}}_2 (\mathbf{Q}_1^{3,1})^{-1}]^{-1}, \tag{7}$$

where $\hat{\mathbf{T}}_2 = \sigma_{O_1 O_2}^1 \mathbf{T}_2 \sigma_{O_2 O_1}^1$. Here, \mathbf{T}_1 and \mathbf{T}_2 are the transition matrices of the host particle and of the inclusion and the matrices $\mathbf{Q}_1^{i,j}$ have the same significance as in [12]. The above result may be generalized in the following way. The case of S_1 containing an arbitrary number of separate inclusions is obtained by inserting the appropriate T-matrix instead of $\hat{\mathbf{T}}_2$. This T-matrix can correspond to an arbitrary number of homogeneous, layered or composite scatterers. Here, we have considered S_1 as the outer surface, imbedded in a homogeneous medium, but outside S_1 there may again be an arbitrary number of consecutive enclosing surfaces. In fact, we can consider any combination of separate and consequently enclosing surfaces. The form of the total T-matrix will be written according to the prescriptions given above.

3. Numerical results

The formulation presented in Section 2 has been implemented in a computer program. The program has two basic units as shown in Fig. 4. The first unit computes the T-matrices for homogeneous, layered and composite scatterers by using localized or distributed sources. These transition matrices can be used to compute the scattering characteristics or as input parameters

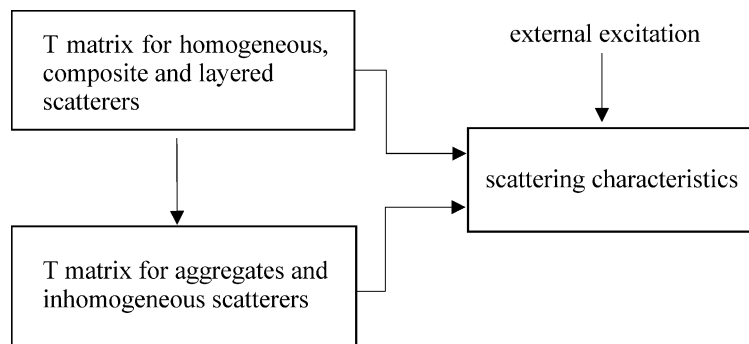


Fig. 4. T-matrix computer program.

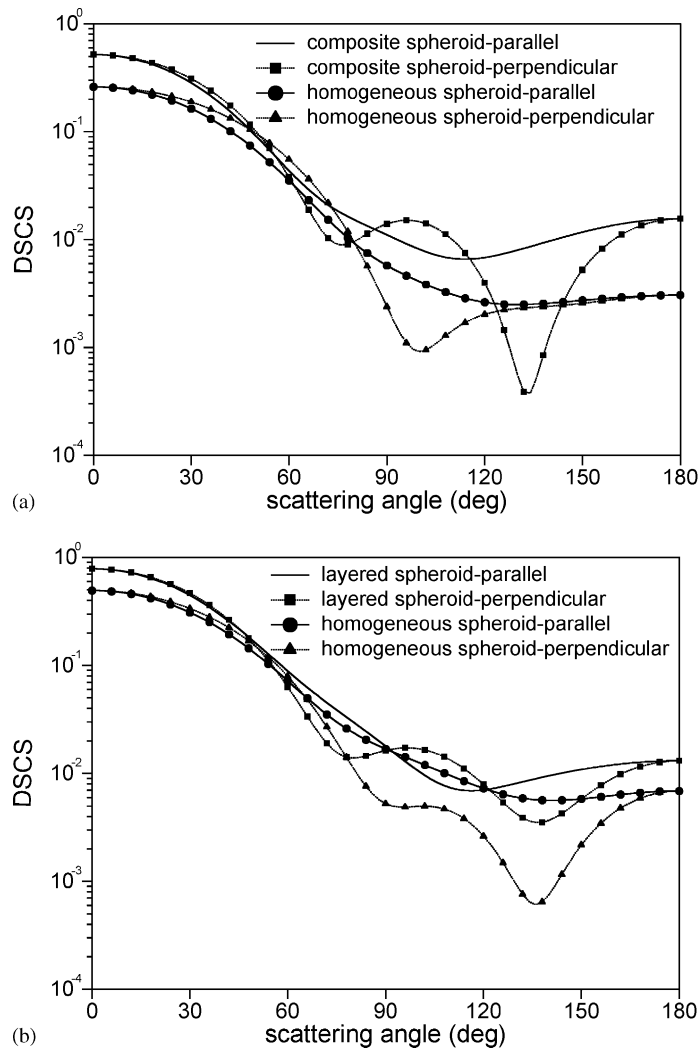


Fig. 5. Differential scattering cross section of (a) a composite, and (b) a layered scatterer together with the results corresponding to homogeneous spheroids with a volume average refractive index. The composite scatterer consists of two half-spheroids with half-axes $a = 0.3 \mu\text{m}$ and $b = 0.2 \mu\text{m}$, and relative refractive indices 1.5 and 1.3. The layered scatterer consists of two concentric spheroids with half-axes $a_1 = 0.3 \mu\text{m}$, $b_1 = 0.2 \mu\text{m}$ and $a_2 = 0.15 \mu\text{m}$, $b_2 = 0.1 \mu\text{m}$, and relative refractive indices 1.5 and 1.8. The volume average refractive indices are 1.4 and 1.538. The external excitation is a plane wave with $\lambda = 0.628 \mu\text{m}$ traveling along the symmetry axis of the scatterers.

for the second unit. In the second unit, the total T-matrix of an arbitrary number of scatterers and the T-matrix of a scatterer containing an arbitrarily shaped inclusion are computed. The geometrical properties of the scatterers and the inclusions can be explicitly defined or they can be given in terms of the T-matrices. The scattering characteristics, as for example the differential scattering cross section and scattering, and extinction and absorption cross sections, are computed by defining the type of the external excitation. The external excitation can be

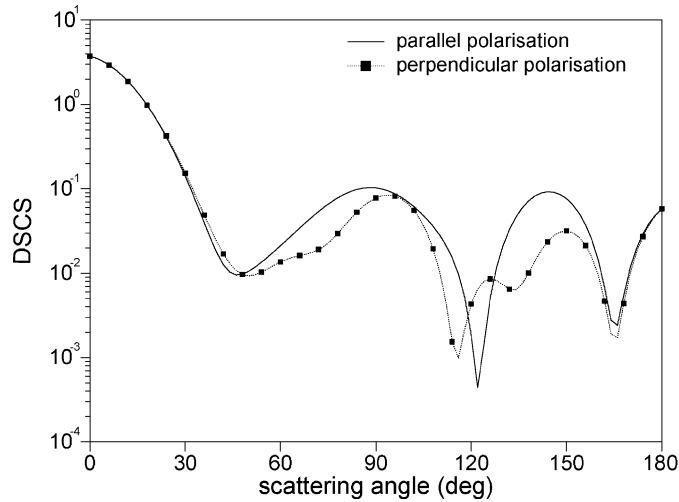


Fig. 6. Differential scattering cross section for the ensemble of composite and layered scatterer. The scatterers are as in Fig. 5. The position of the composite scatterer is given with respect to a global coordinate system by $x = y = z = 0.3 \mu\text{m}$, and the orientation by $\alpha = \beta = 45^\circ$. For the layered scatterer, we choose $x_1 = y_1 = z_1 = -0.3 \mu\text{m}$ and $\alpha_1 = \beta_1 = 0^\circ$. The plane wave ($\lambda = 0.628 \mu\text{m}$) travels along the z -axis of the global coordinate system and the scattering characteristics are computed in the azimuthal plane $\varphi = 0^\circ$.

a plane wave, a Gaussian beam or a dipole. Parenthetically, we note that our computer code enables us to compute the T-matrix of chiral and anisotropic scatterers.

In our simulation, we consider a composite and a layered prolate spheroid. The composite scatterer consists of two identical half-spheroids with relative refractive indices (with respect to the ambient medium) 1.5 and 1.3. The half-axes of the composite scatterer are $a = 0.3 \mu\text{m}$ and $b = 0.2 \mu\text{m}$. The layered scatterer consists of two concentric prolate spheroids with relative refractive indices 1.5 and 1.8. The half-axes of the spheroids are $a_1 = 0.3 \mu\text{m}$, $b_1 = 0.2 \mu\text{m}$ and $a_2 = 0.15 \mu\text{m}$, $b_2 = 0.1 \mu\text{m}$. In our simulation we choose the external excitation to be a plane wave with $\lambda = 0.628 \mu\text{m}$. The direction of propagation of the incident wave is along the symmetry axis of the scatterers. In Fig. 5, we show the differential scattering cross sections normalized by πa^2 . Also shown are the results corresponding to homogeneous spheroids with volume average refractive indices 1.4 and 1.538, respectively.

The results plotted in Fig. 6 show the differential scattering cross section normalized by πa^2 for the ensemble of composite and layered scatterer. The position of the composite scatterer is given with respect to a global coordinate system by the Cartesian coordinates $x = y = z = 0.3 \mu\text{m}$, while the orientation is given by the Euler angles $\alpha = \beta = 45^\circ$. For the layered scatterer we choose $x_1 = y_1 = z_1 = -0.3 \mu\text{m}$ and $\alpha_1 = \beta_1 = 0^\circ$. The incident wave travel along the z -axis of the global coordinate system and the scattering characteristics are computed in the azimuthal plane $\varphi = 0^\circ$. The total T-matrix is computed according to (6) by using the T-matrices of the individual scatterers.

Next, we use this matrix as input parameter for the program unit which computes the T-matrix of an inhomogeneous scatterer. The host particle is spherical with a radius of $r = 0.8 \mu\text{m}$ and a refractive index of $m = 1.2$. Thus, the resulting T-matrix corresponds to a sphere containing a

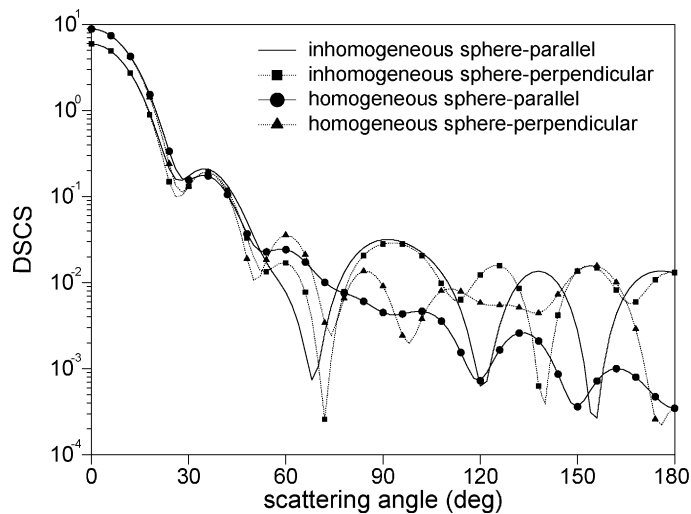


Fig. 7. Differential scattering cross section of a sphere containing a composite and a layered spheroid as separate inclusions. The radius of the host sphere is $r = 0.8 \mu\text{m}$ and the refractive index is $m = 1.2$. The positions of the composite and the layered spheroid are given with respect to the center of the sphere as in Fig. 6. Also shown are the results corresponding to a homogeneous sphere with a volume average refractive index of 1.22.

composite and a layered spheroid as separate inclusions. The differential scattering cross section for the inhomogeneous scatterer is shown in Fig. 7 together with the results corresponding to a homogeneous sphere with a volume average refractive index of 1.22.

4. Conclusions

In this paper, a T-matrix formalism for complex structures has been presented. The method combines results concerning the T-matrix calculations for homogeneous, layered and composite scatterers with basic results on T-matrix calculations for an arbitrary number of scatterers and inhomogeneous scatterers. The T-matrix can be computed by using localized or distributed sources. This improves the performance of the T-matrix method for solving a large class of boundary-value problems in electromagnetic scattering theory.

Acknowledgements

The support of Deutsche Forschungsgemeinschaft is gratefully acknowledged.

References

- [1] Waterman PC. Symmetry, unitarity and geometry in electromagnetic scattering. *Phys Rev* 1971;D3:825–39.
- [2] Mishchenko MI, Hovenier JW, Travis LD. Light scattering by nonspherical particles. Theory, measurements and applications. San Diego: Academic Press; 2000.

- [3] Boström A. Scattering of acoustic waves by a layered elastic obstacle immersed in a fluid: An improved null field approach. *J Acoust Soc Am* 1984;76:588–93.
- [4] Iskander MF, Lakhtakia A, Durney CH. A new procedure for improving the solution stability and extending the frequency range of the EBCM. *IEEE Trans Antennas Propag* 1983;AP-31:317–24.
- [5] Bates RHT, Wall DJN. Null field approach to scalar diffraction: I. General method; II. Approximate methods; III. Inverse methods. *Philos Trans Roy Soc London A* 1977;287:45–117.
- [6] Lakhtakia A, Iskander MF, Durney CH. An iterative EBCM for solving the absorption characteristics of lossy dielectric objects of large aspect ratios. *IEEE Trans Microwave Theory Tech* 1983;MTT-31:640–7.
- [7] Hackman RH. The transition matrix for acoustic and elastic wave scattering in prolate spheroidal coordinates. *J Acoust Soc Am* 1984;75:35–45.
- [8] Schulz FM, Stamnes K, Stamnes JJ. Scattering of electromagnetic waves by spheroidal particles: a novel approach exploiting the T matrix computed in spheroidal coordinates. *Appl Opt* 1998;37:7875–96.
- [9] Wriedt T, Doicu A. Formulations of the EBCM for three-dimensional scattering using the method of discrete sources. *J Mod Opt* 1998;45:199–213.
- [10] Doicu A, Eremin Y, Wriedt T. *Acoustic and electromagnetic scattering analysis using discrete sources*. London: Academic Press; 2000.
- [11] Peterson B, Ström S. T matrix for electromagnetic scattering from an arbitrary number of scatterers and representations of E(3). *Phys Rev D* 1973;8:3661–78.
- [12] Peterson B, Ström S. T-matrix formulation of electromagnetic scattering from multilayered scatterers. *Phys Rev D* 1974;10:2670–84.
- [13] Ström S, Zheng W. The null field approach to electromagnetic scattering from composite objects. *IEEE Trans Antennas Propag* 1988;36:376–82.
- [14] Doicu A, Wriedt T. Calculation of the T-matrix in the null-field method with discrete sources. *J Opt Soc Am A* 1999;16:2539–44.
- [15] Doicu A, Wriedt T. Extended boundary condition method with multipole sources located in the complex plane. *Opt Commun* 1997;139:85–91.
- [16] Doicu A, Wriedt T. Null-field method with discrete sources to electromagnetic scattering from composite scatterers. *Opt Commun* 2001;190:13–4.
- [17] Doicu A, Wriedt T. Null-field method with discrete sources to electromagnetic scattering from layered scatterers. *Comput Phys Commun*, in press.